Ultra-Sensitive Cascaded Integrated Photonic Ultrasound Transducers (IPUTs)

Van Neer, P. L.M.J.; Harmsma, P. J.; Gerritsma, A. M.; Altmann, R. K.; Valappil, S. V.; Oderwald, M. P.; Piras, D.; Quesson, B. A.J.; Verweij, M. D.; More Authors

DOI
10.1109/UFFC-JS60046.2024.10793785

Publication date
2024

Document Version
Final published version

Published in
2024 IEEE Ultrasonics, Ferroelectrics, and Frequency Control Joint Symposium (UFFC-JS)

Ultra-Sensitive Cascaded Integrated Photonic Ultrasound Transducers (IPUTs)

P.L.M.J. van Neer[1], P.J. Harmsma[2], A.M. Gerritsma[1], R.K. Altmann[2], S.V. Valappil[3], M.P. Oderwald[2], D. Piras[4], B.A.J. Quesson[1], S. Bhat[5], M. Harjanne[5], S. Ylinen[5], Y. Marin[5], P. Heimala[5], T.H. Jansen[2], M.D. Verweij[3], M.S. van der Heiden[1]

[1]*Department of Acoustic Sensor & Sonar Systems, TNO, the Hague, the Netherlands*
[2]*Department of Optics, TNO, Delft, the Netherlands*
[3]*Medical Imaging, ImPhys, Delft University of Technology, the Netherlands*
[4]*Department of Acoustic Signatures and Noise Control, TNO, the Hague, the Netherlands*
[5]*VTT, Technical Research Ctr. of Finland Ltd., Espoo, Finland*
paul.vanneer@tno.nl

2024 IEEE Ultrasonics, Ferroelectrics, and Frequency Control Joint Symposium (UFFC-JS) | 979-8-3503-7190-1/24/$31.00 ©2024 IEEE | DOI: 10.1109/UFFC-JS60046.2024.10793785

***Abstract*—Echography is an important medical diagnostic technique. Historically, the key improvement driver was the hypothesis that higher image quality leads to better diagnoses and increased patient health. Here, a major parameter is the signal to noise ratio (SNR). Diffraction and attenuation reduce pressure levels during propagation. Thus, an SNR increase yields detection at larger depths benefitting traditionally difficult to image patients (eg large/obese patients). Peak pressures are limited by safety standards (mechanical/thermal index). Thus, to increase SNR more sensitive transducers are required. The state of the art Noise Equivalent Pressure (NEP) for piezotransducers / cMUTs / pMUTs is ~0.5 Pa at 1 MHz [1,2,3]. A recent innovation is the Integrated Photonic Ultrasound Transducer (IPUT), which combines a membrane and a photonic waveguide to measure ultrasound waves. Literature [5] reported such a device producing a 0.38 Pa NEP at 0.47 MHz and 21% -6 dB bandwidth with a 169x smaller spatial footprint compared to 0.5 x 0.5 wavelength². Here, we cascade IPUTs into array elements and transform IPUT sensitivity per area into high absolute sensitivity. Several transducer elements were created by cascading up to 16 IPUTs. After designing these devices, their performance was predicted, and subsequently they were fabricated via VTT's 3 µm thick silicon-on-insulator (SOI) waveguide platform. IPUT performance was measured in a water tank using a custom calibrated source transducer. The transfer functions and noise of each signal chain component was measured and analyzed. The results showed for a 5 cascaded IPUT element a measured NEP of 4 mPa at 0.54 MHz with a 13% -6 dB bandwidth. This improves on the state-of-the-art by a factor of 90-116x.**

Keywords*—Integrated Photonic Ultrasound Transducer (IPUT), transducer, noise equivalent pressure (NEP), signal to noise ratio (SNR)

I. INTRODUCTION

Echography is an important medical diagnostic technique. Historically, the key improvement driver was the hypothesis that a higher image quality leads to better diagnoses and therefore increased patient health. Here, a major parameter is the signal-to-noise-ratio (SNR). During propagation the signal level is reduced by diffraction and attenuation effects. Thus, an increase in SNR yields improved detection at larger depths, which benefits traditionally difficult to image patients (eg large/obese patients). The allowable peak pressures are limited by safety standards (mechanical/thermal index). Thus, more sensitive transducers are needed to increase the SNR. The state-of-the-art (SOTA) noise equivalent pressure (NEP) for piezotransducers / capacitive Micromachined Ultrasound Transducers (cMUTs) / piezoelectric Micromachined Ultrasound Transducers (pMUTs) is ~0.5 Pa at 1 MHz [1,2,3]. A recent innovation is the Integrated Photonic Ultrasound Transducer (IPUT), which combines a membrane and a photonic waveguide to measure ultrasound. If an acoustic wave displaces the membrane, the refractive index or shape/length of the photonic waveguide is altered. This modifies the optical transfer function of the photonic waveguide, which can be measured in a variety of ways [4,5,6]. Ouyang et al. [5] reported on a Mach Zehnder Interferometer based IPUT (MZI-IPUT). Here, the sensing arm of a Mach Zehnder Interferometer is routed over a membrane and whereas the reference arm is not. An interferometric concept is used to measure the phase difference between the sensing and reference arms. A schematic image of an MZI-IPUT is shown in Fig. 1.

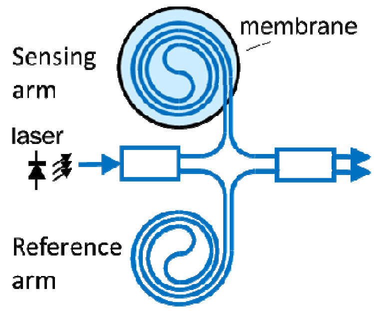

Fig. 1. Schematic of an MZI-IPUT.

An MZI-IPUT was shown in literature to produce a 0.38 Pa NEP at 0.47 MHz and 21% -6 dB bandwidth with a 169x smaller spatial footprint compared to 0.5 x 0.5 acoustical wavelength² [5]. Unfortunately, in most acoustical applications there is no advantage to make the transducer dimensions smaller than 0.5 acoustical wavelength. Hence, to truly demonstrate the advantages of IPUTs we must transform the high IPUT sensitivity per unit area into high absolute sensitivity. In this work, we cascade multiple IPUTs into acoustic elements and demonstrate the higher sensitivity by measuring the reduced Noise Equivalent Pressure (NEP).

II. Simulation and Experimental Setup

A. IPUT design

IPUTs were designed and their performance predicted using custom analytical models, COMSOL (COMSOL BV, Zoetermeer, the Netherlands) FEM (mechanics) and FIMMWAVE (Photonics Design, Oxford, United Kingdom) (photonics) and fabricated using VTT's low-loss 3 µm thick Silicon-On-Insulator (SOI) waveguide platform [8]. The IPUTs had: an oxide membrane thickness of 2.6 µm, a radius of 0.05 mm, a center frequency of ~0.6 MHz, and 4 optical waveguide loops/membrane with silicon waveguide cross-section 1.5 x 3 µm^2. The spiral waveguide trajectory utilized Archimedean spiral and Euler bends [9] and it was carefully designed to minimize the excitation of higher order modes in long tight spirals.

Several transducer elements were created by cascading up to 16 IPUTs. Fig. 2 shows a schematic of 3 IPUTs cascaded into a single acoustic element.

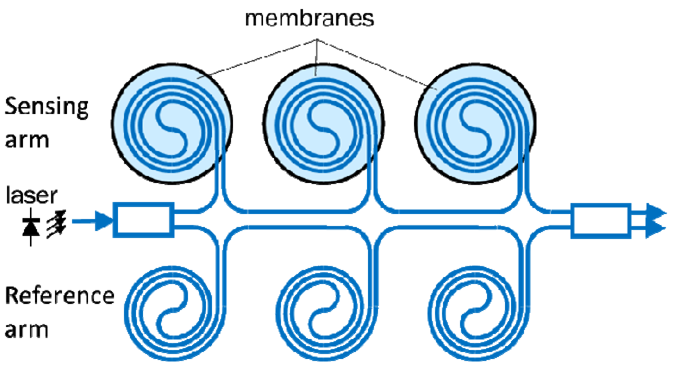

Fig. 2. Image of a transducer element created by cascading 16 IPUTs.

Fig 3 shows an image of a produced acoustic element created by cascading 16 IPUTs.

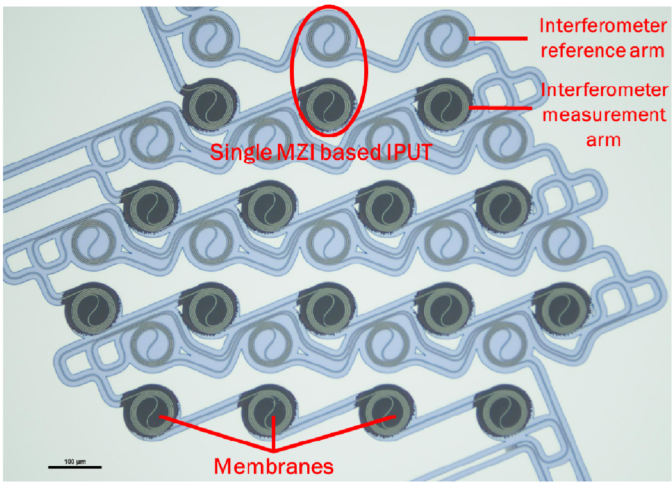

Fig. 3. Image of a transducer element created by cascading 16 IPUTs.

B. Measurement setup

IPUT performance was measured in a water tank using a custom calibrated source transducer. A schematic of the experimental setup is shown in Fig. 4.

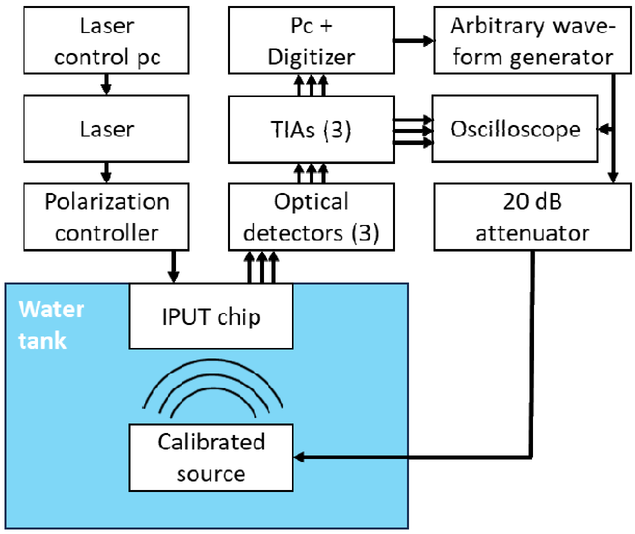

Fig. 4. Schematic of the experimental setup.

Two circular single element calibrated sources were used: an Imasonic, type 13579 250 kHz transducer and a 1 MHz Panametrics V303 transducer. The sources were calibrated using the methodology described in [7]. During the calibration the cables were marked and the voltage on the transducer clamps was measured using an electrical probe. The same cables were used in the setup during the actual measurements. The beam profiles of the calibrated transducers were measured and compared to analytical diffraction functions. The IPUT chip was mounted in an XYZ stage and aligned on-axis with the calibrated source. The distance between the IPUT chip and the calibrated source was 27 cm (the far field). The temperature of the water was measured. The pressure impinging on the IPUT chip was calculated by multiplying the voltage on the calibrated source with its transmit transfer function and correcting for diffraction and attenuation.

Each of the 3 optical 3x3 interferometer outputs was analyzed individually at the level of the digitizer (i.e. no corrections were made for the TransImpedance Amplifiers (TIA)). Therefore, all noise contributions of the entire optical signal chain were present.

The calibrated source transducer was excited with single cycle sine signals with progressively lower amplitudes (5 Vp – 1 mVp). For each voltage level 1000 traces were recorded. The averaged trace was used to determine the -6 dB bandwidth and to obtain the time region T_{sig} in which the acoustic signal would arrive. To determine the NEP only single traces (so no averages) were used. To determine the received signal level the maximum of the absolute signal within time region T_{sig} was used. The Root Mean Square (RMS) noise level was calculated based on the same trace in a noise time window T_{noise} located before time region T_{sig} containing the acoustic signals.

We define the Noise Equivalent Pressure (NEP) as:

$$NEP = Noise_{RMS} / sensitivity \quad (1)$$

We define the practical NEP as:

$$NEP = 4*Noise_{RMS} / sensitivity \quad (2)$$

III. Results and Discussion

Fig. 5 displays the measured amplitude vs applied pressure for an acoustic element consisting of 5 cascaded IPUTs. The signal amplitude and the RMS noise level are denoted by the blue circles and red crosses, respectively. We would like to stress that no averaging has been used to obtain this data. The yellow horizontal line indicates 4x the mean RMS noise level – the level above which we could visually detect the signals in the single digitizer traces. The dashed purple is a linear fit to the signal amplitudes above 4x the mean RMS noise level.

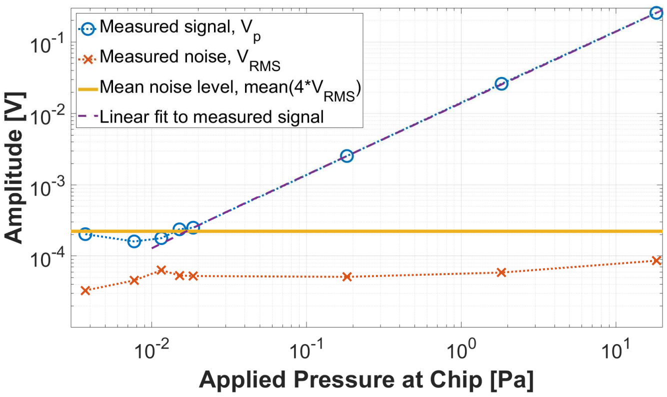

Fig. 5. Measured signal amplitude vs applied pressure for an acoustic element consisting of 5 cascaded IPUTs. The signal amplitude and the RMS noise level are denoted by the blue circles and red crosses, respectively. The yellow horizontal line indicates 4x the mean RMS noise level (the level above which we could detect the signals by eye), whereas the dashed purple is a linear fit to the signal amplitudes above 4x the mean RMS noise level.

The results shown in Fig. 5 indicate that the measured NEP was 4 mPa at 0.54 MHz with a 13% -6 dB bandwidth. The practical NEP (at $4*V_{RMS}$ noise) was 17 mPa. The element signal level increased linearly with higher pressures applied to the chip.

Fig. 6 shows the peak-to-peak optical wavelength shift as a function of the number of IPUTs cascaded per acoustic element. The source transducer was aligned such that the maximum pressure fell on the chip, and said transducer was excited by a 1 cycle sine with an amplitude of 1V.

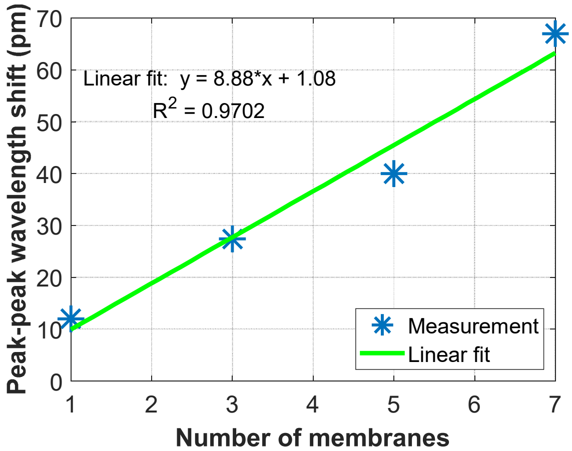

Fig. 6. The peak-to-peak optical wavelength shift as a function of the number of IPUTs cascaded per acoustic element.

As can be seen from Fig. 6 the optical wavelength shift roughly linearly increases for increasing numbers of IPUTs cascaded per acoustic element (R^2 linear fit = 0.97).

In Table 1 the performance of the TNO acoustic element based on 5 cascaded IPUTs including optical read-out equipment is compared to the state-of-the-art (SOTA) reported in literature regarding a piezomaterial / cMUT / pMUT based matrix array element including dedicated optimized electronics. The table also reports the performance of the SOTA IPUT-like devices including optical read-out.

Table I Comparison of NEP, $NEP_{PRATICAL}$, center frequency and bandwidth for TNO element based on 5 cascaded IPUTs and various state-of-the-art (SOTA) devices reported in literature

		SOTA [1,2,3]	*Leinders et al. [4]*	*Ouyang et al. [5]*	*TNO, 5 cascaded*
Type		Piezo/cMUT/ pMUT	RR IPUT	MZI IPUT	MZI IPUT
NEP	[Pa]	0.50	0.40	0.38	0.0043
$NEP_{practical}$	[Pa]	2.0	1.60	1.52	0.017
Center frequency	[MHz]	1	0.76	0.47	0.54
-6 dB bandwidth	[%]	80	19	21	13

Table 1 shows that both the NEP and $NEP_{practical}$ of the TNO acoustic element based on 5 cascaded IPUTs is improved by a factor of ~90x compared to the devices reported by Leinders et al. [4] and Ouyang et al. [5] taking into account the available spatial footprint of a matrix array element of 0.5 x 0.5 wavelength^2. Compared to the SOTA piezo/cMUT/pMUT solutions reported in the literature, the acoustic element based on 5 cascaded IPUTs has a NEP which is improved by a factor of 116x. It should be noted that the -6 dB bandwidth of the IPUT devices reported in Table 1 is between 13-21% and therefore significantly lower than the 80% -6 dB bandwidth typically required for medical imaging applications.

IV. Summary/Conclusion

In this work we have demonstrated that one can cascade multiple IPUTs to form a single acoustic element and through that transform the high IPUT sensitivity per area into high absolute sensitivity per acoustic element (90-116x improved compared to SOTA). We have demonstrated this by measuring the NEP and the $NEP_{practical}$ and comparing these to results reported in literature for other sensor types. The measured peak-to-peak optical wavelength shift increased linearly with the number of cascaded IPUTs. Since in our measurements the limiting factor with respect to the noise level was the noise produced by the optical detector and the preamplifier, this meant that the NEP dropped linearly with the number of IPUTs cascaded for a single acoustic element. The optical signal quality deteriorated for more than 7 cascaded IPUTs - our hypothesis is the progressively increased excitation of higher order waveguide modes. In case even larger numbers of IPUTs could be cascaded per acoustic element, we expect the NEP drop as a function of the number of IPUTs per acoustic element to deviate from linearity, if the noise produced by the IPUTs themselves becomes dominant. In the future we will work at improving the -6 dB bandwidth whilst maintaining the low NEP, taking cues from the lessons learned from the pMUT/cMUT literature (also membrane based devices).

Acknowledgment

This work has been supported by the TNO Early Research Program (ERP) ‘Opto-acoustics’, NWO grant NWA-1160.18.095 ‘Opto-acoustic sensor and ultrasonic microbubbles for dosimetry in proton therapy’, and EU grant 101092947 ‘Medical Integrated Photonic Ultrasound Transducer’.

References

[1] W. Xia, et. al., "An optimized ultrasound detector for photoacoustic breast tomography," Medical physics, no. 032901, 2013.

[2] R. Manwar, et. al., "Overview of Ultrasound Detection Technologies for Photoacoustic Imaging," Micromachines, vol. 11, no. 7, p. 692, 2020.

[3] A. Kashani Ilkhechi, et.al., "Transparent capacitive micromachined ultrasonic transducer (CMUT) arrays for real-time photoacoustic applications," Optics Express, vol. 28, no. 9, pp. 13750-13760, 2020.

[4] S.M. Leinders, et.al., "A sensitive optical micro-machined ultrasound transducer (OMUT) based on a silicon photonic ring resonator on an acoustical membrane," Nature Scientific Reports, 14328, 2015.

[5] B. Ouyang, et.al., "On-chip silicon Mach-Zehnder interferometer sensor for ultrasound detection," Optics Letters, vol. 44, no. 8, pp. 1928-1931, 2019.

[6] W.J. Westerveld, et. al., "Sensitive, small, broadband and scalable optomechanical ultrasound sensor in silicon photonics," Nature Photonics, vol. 15, pp. 341-345, 2021.

[7] P.L.M.J. van Neer, et al., ‘Transfer functions of US transducers for harmonic imaging and bubble responses’, Ultrasonics, 46:336-340, 2007.

[8] T. Aalto, et al., ‘Open-access 3 µm SOI waveguide platform for dense photonic integrated circuits’, IEEE Journal of Selected Topics in Quantum Electronics, vol. 25, no. 5, pp. 1-9, Sept.-Oct. 2019, Art no. 8201109.

[9] M. Cherchi, et. al., ‘Dramatic size reduction of waveguide bends on a micron-scale silicon photonic platform,’ Optics Express, vol 21, pp. 17814-17823, 2013.